# Magnetic order from molecular oxygen anions

Riyadi, Syarif

Chapter 1

# Introduction

## 1.1 General Introduction

The word "magnet" comes from the Magnetes, a tribe living during ancient Greek history in Magnesia ad Sipylum (modern Turkey). The first magnets in the world are believed to have been found in this region, at mount Sipylus [1]. In Greek these magnets are called magntis lithos ($\mu\alpha\gamma\nu\eta\tau\iota\zeta\lambda\iota\theta\phi\zeta$), which means magnesian stone, commonly known as lodestone.

> *"That stone not only attracts iron rings, but imparts to them a similar power of attracting other rings; and sometimes you may see many pieces of iron and rings suspended from one another to form quite a long chain" -Socrates (470-399 BC)-*

Curiosity in magnetism started with the discovery of lodestone. In the $4^{th}$ century the compass was invented in China, to this day the simplest use of magnetic materials. Originally lodestone was used to magnetize a piece of iron in the compass, which aligns according to the earth's magnetic field. Afterwards, some part of the world's civilization became focused on magnetism and magnetic materials. People began to consider the use of magnetic materials in everyday life.

Following the discovery of the electron spin in the early $20^{th}$ century [2–4], scientific research into magnetic materials grew rapidly. Investigation of the magnetic properties of materials and the synthesis of new materials with interesting magnetic properties that are also useful for technological applications is an active research area. For example, the use of ferromagnetic materials in storage devices is perhaps the most obvious implication of magnetic materials in modern nanotechnology.

Ferromagnetic metals, mainly transition metal elements, are used for spin-injection, a technique widely used in device applications of today such as storage

and memory devices [5–7]. Transition metals are chosen due to their high spin polarization and high electron density at the Fermi level (conductivity). Magnetism in transition metal elements originates from unpaired electrons in the 3d orbitals. Fascinating properties spanning from the simplest mechanisms such as ferromagnetism or antiferromagnetism to more complex physics such as superconductivity or multiferroicity can emerge from compounds and alloys containing transition metals [8–10].

Magnetism in materials based on 3d- and 4f-electron systems is mostly well studied. On the other hand, magnetism based on p-electron materials is less researched, although there are reports on such systems, hereafter referred to as "$d^0$ magnetism". For example, Rajca et al. and Zaidi et al. have reported the synthesis of magnetic organic polymers [11, 12]. Room temperature ferromagnetism in $HfO_2$ is probably the most remarkable report in the field of inorganic $d^0$-magnetism [13]. There are also recent reports on ferromagnetism in nano-crystals of various materials that are non-magnetic in bulk form [14, 15]. However, the small number of papers on these types of materials might indicate poor experimental reproducibility. Various forms of carbon have been reported to exhibit $d^0$-magnetism [16–22]. Of particular current interest is that magnetic moments can be introduced in carbon layers (graphene) by creating defects [23]. Moreover, the detection of spin transport in single carbon layers (graphene) placed between two ferromagnetic cobalt electrodes has been demonstrated [24]. The low spin-orbit coupling of 2p-electron materials such as carbon is advantageous for spin-injection experiments because spin decoherence effects are small. This is different from heavier elements such as transition metals where the greater nuclear charge results in higher spin-orbit coupling and greater decoherence effects on polarized spins.

As one of the candidate $d^0$-magnetic materials, molecular oxygen offers promising properties. The magnetic structure of molecular oxygen has been thoroughly discussed [25, 26]. Furthermore, superconductivity in molecular oxygen was observed at high pressure and low temperature [27]. Research on alkali metal oxides containing molecular oxygen anions (peroxide and superoxide) was already started in the early $20^{th}$ century [28, 29]. However, due to the limited experimental techniques available, studies at that time were restricted to the comparison of chemical compositions, colors and chemical reactivity. Detailed discussions on the magnetic properties of the alkali metal superoxides ($AO_2$; A = Na, K, Rb, Cs) started in the late 1950's. Following earlier reports, authors started to correlate the magnetism with the crystallographic properties of the materials. A detailed study of rubidium sesquioxide ($Rb_4O_6$) in 1991 started a new chapter on the intriguing physical properties of alkali metal oxides [30]. Attema et al. then predicted half-metallicity in $A_4O_6$ [31, 32]. However, these theoretical studies have thus far not been confirmed by experimental results. Fortunately, this has initiated further research on these types of magnetic materials (anionogenic magnets). There have been a considerable number of reports on alkali metal oxides in the last 4 years, both on theoretical and experimental studies.

In this thesis I will discuss the possibilities provided by the magnetic properties of alkali metal oxides. Attempts to explore new phases will be discussed. The content focuses mainly on $RbO_x$ phases and $CsO_2$. I show that it is possible to continuously vary the oxygen content in $RbO_x$ compounds. Some attempts to explore new phases of $CsO_x$ and $KO_x$ are briefly described in the last part of the thesis, together with a discussion on $RbO_x$ thin films. This thesis contributes to knowledge of both the physics and chemistry of alkali metal oxides.

## 1.2 Alkali Metal Oxides and their Properties

### 1.2.1 Molecular Oxygen Species and Alkali Metal Oxide Compounds

Figure 1.1 depicts molecular orbital diagrams of molecular oxygen species. Molecular oxygen ($O_2$) has 2 unpaired electrons and is thus paramagnetic, ordering antiferromagnetically below 24 K. It becomes superconducting at very low temperature and high pressure [27]. A comprehensive study on the properties of molecular oxygen is given by Freiman and Jodl [33]. Ionization of $O_2$ leads to the removal of 1 electron from the $\pi^*$ orbital, forming the magnetic dioxygenyl ($O_2^+$) cation. This species can only be stabilized by the $MF_6^-$ anion (M = Sb, Pt). With an addition of 1 electron in the $\pi^*$ orbital of $O_2$, another magnetic form of molecular oxygen, called superoxide (S = 1/2 system), is formed. Adding one more electron to the same orbital, the non-magnetic peroxide anion is formed.

Alkali metals can easily bond with molecular oxygen and form ionic salts ($A_2O_2$, $A_2O_3$, $AO_2$). Due to their high sensitivity to moisture, the handling and the oxidation of alkali metals can be very difficult. At the lowest oxygen content, alkali metals form bronze-colored metallic sub-oxides ($A_6O$, $A_9O_2$, etc.), whereas yellow alkali metal superoxides can be synthesized by long oxidation of the alkali metals. Intermediate phases such as alkali metal peroxides and sesquioxides ($A_2O_2$, $A_2O_3$) can be obtained by careful oxidation of the alkali metals. The scheme below represents the oxidation stages of alkali metal oxides:

Sub-oxides ($A_6O$, $A_9O_2$, etc.) $\longrightarrow$ Oxide ($A_2O$) $\longrightarrow$ Peroxide ($A_2O_2$) $\longrightarrow$ Sesquioxide ($A_2O_3$) $\longrightarrow$ Superoxide ($AO_2$)

The more oxidized compounds above are in general insulating ionic salts ($A_2O$, $A_2O_2$, $A_2O_3$, $AO_2$). Alkali metal oxides ($A_2O$) are often described as transparent insulating materials. However, the colors of these materials vary across the series. Based on the synthesis attempts described in subsequent chapters, $K_2O$ is a red-brick colored compound, whereas $Rb_2O$ has a dark green to yellow color. $Cs_2O$ is correctly described in the literature as a yellow to orange colored material [34]. The peroxides ($A_2O_2$) and superoxides ($AO_2$) have the same color for each alkali metal, white for the former and yellow for the latter. The existence of the sesquioxides ($A_2O_3$) has been a matter of debate. The existence of $Rb_2O_3$ and $Cs_2O_3$ has been

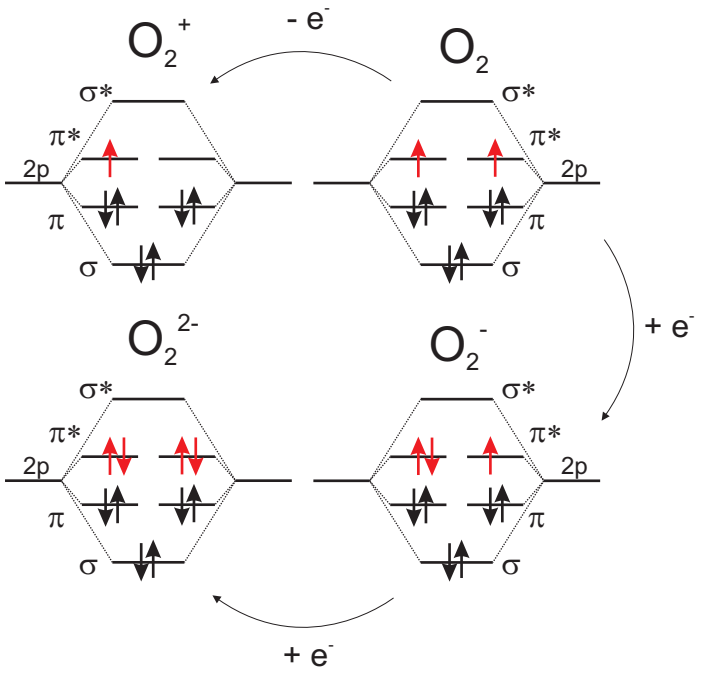


Figure 1.1. Molecular oxygen species: dioxygenyl ($O_2^+$), molecular oxygen ($O_2$), superoxide ($O_2^-$), and peroxide ($O_2^{2-}$).

confirmed and they can be synthesized by solid state reaction [35], but the existence of $K_2O_3$ and $Na_2O_3$ has not yet been confirmed (chemically or structurally). It has been reported that $K_2O_3$ is a brick-red colored compound [36].

Among all the alkali metal oxide phases, only those containing superoxide anions can exhibit magnetic behavior (Figure 1.1). Both molecular oxygen ($O_2$) and $AO_2$ are well known to be antiferromagnets at low temperature, whereas $A_2O_2$ are non-magnetic. Different crystal structures of molecular oxygen at low temperatures and high pressures have been identified, all of which have parallel molecules and give rise to antiferromagnetic ordering [26, 37]. It is reported that $KO_2$, $RbO_2$, and $CsO_2$ have Neel temperatures ($T_N$) of 7 K, 15 K, and 9.6 K [38].

### 1.2.2 Phase Transitions in Alkali Metal Superoxides

The crystal structures of $AO_2$ are all derived from rocksalt, and the orientation of the oxygen dumbbells determines the structure. The structure of $AO_2$ (A = K, Rb, Cs) at room temperature is tetragonal ($a = b \neq c$, space group: $I4/mmm$). In this structure the superoxide dumbbells are on average pointing in the $c$-direction, leading to a longer $c$-axis (see Figure 1.2(a)). The unit cell volume depends on the size of the cation (the ionic radius increases with atomic number; $r_{Cs} > r_{Rb} > r_K$).

At room temperature, thermal activation results in precession of the dumbbells around the $c$-axis. Similarly, the disordered pyrite (cubic) structure of $NaO_2$ (space group: $Fm\bar{3}m$) at room temperature is attributed to spherical disorder of the superoxide orientations (see Figure 1.2(b)) [39].

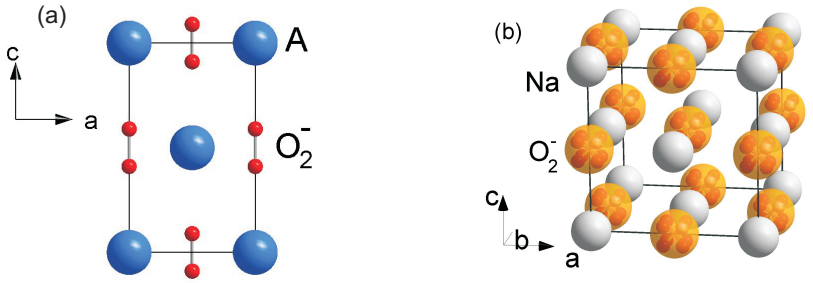


Figure 1.2. (a) The $ac$-plane view of $AO_2$ (tetragonal) at room temperature (A = K, Rb, Cs); (b) Room temperature disordered-pyrite (cubic) $NaO_2$ (space group: $Fm\bar{3}m$).

The low temperature structures of single crystals of $AO_2$ have been studied [40], although details are lacking. All $AO_2$ show a sequence of crystallographic phase transitions below room temperature. The phase transitions at low temperatures in $NaO_2$ and $KO_2$ were first reported by Todd in 1953 from heat capacity measurements [41]. $NaO_2$ transforms to an ordered-pyrite structure below 223 K (space group: $Pa\bar{3}$), in which the superoxide orientations are ordered along the [111] directions of the cubic unit cell, and further transforms to the orthorhombic marcasite structure below 196 K [42]. Long-range antiferromagnetic order in $NaO_2$ is reported to appear at 43 K, above which antiferromagnetic short-range order might exist up to ∼200 K. The room-temperature tetragonal structure of $KO_2$ is only an average structure. There are thought to be small shifts and tilts of the dumbbells away from the $c$-axis, which are correlated over short length scales to give small orthorhombic domains. This was inferred from the appearance of incommensurate superstructure reflections in single crystal x-ray diffraction [43]. Below 196 K the anions tilt by ∼20° away from the $c$-axis to give a monoclinic structure, which becomes triclinic below 9.6 K (the antiferromagnetic phase transition). The other alkali metal superoxides ($RbO_2$ and $CsO_2$) also undergo a series of crystallographic phase transitions at low temperatures [42]. Similar to $KO_2$, the room temperature tetragonal structure of $RbO_2$ is thought to be an average structure which is composed of many orthorhombic domains, with a short-range coherent superstructure due to dumbbell shifts and tilts. An average orthorhombic distortion sets in at ∼150 K and persists down to 70 K, where a monoclinic structure appears and remains down to the lowest temperatures measured. The structure of $CsO_2$ at low temperature is simpler. From single-crystal x-ray diffraction it was observed that tetragonal $CsO_2$ transforms to an orthorhombic phase below 190 K.

The structure stays orthorhombic into the magnetically ordered phase below 9 K. Details of the orthorhombic and monoclinic phases of $RbO_2$ and $CsO_2$ other than the unit cell parameters are not known, but distortions from the room-temperature tetragonal structure are much smaller than in $KO_2$.

The re-orientation of the dumbbells in $AO_2$ induces lattice distortion/symmetry change. The driving force for dumbbell reorientation from the cubic (A = Na) or tetragonal phase (A = K, Rb, Cs) is a lowering in energy provided by breaking the degeneracy of the $\pi^*$ orbitals of the superoxide anion. The filled $\pi^*$ orbital is lowered in energy, resulting in a decrease in total energy. As an example, in $KO_2$ the anions are aligned along $c$ in the high-temperature tetragonal $I4/mmm$ structure, with point group $D_{4h}$. The point-group symmetry of the anion site must be lowered in order to lift the orbital degeneracy [44]. This occurs when the anion dumbbells are slightly tilted from the $c$-axis. Additionally, the $K^+$ cations are thought to undergo spatial displacement perpendicular to the $c$-axis. Thus, the dumbbells encounter additional change in the potential energy, resulting in a lateral shift of their positions. As mentioned above, short-range correlation of these tilts and shifts seemingly leads to an incommensurate structure. Similar to $KO_2$, the phase transition in $NaO_2$ from the ordered-pyrite structure (cubic symmetry, dumbbells point along the [111] directions) to the marcasite structure (orthorhombic) at 196 K involves removing the orbital degeneracy of the superoxide anions [45].

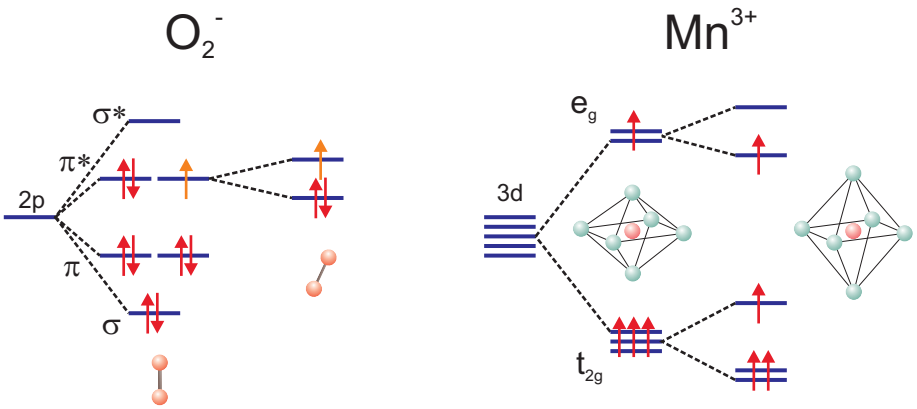


Figure 1.3. Schematic representation of Jahn-Teller effect in alkali metal superoxides (left). This is analogous to the Jahn-Teller effect in manganite perovskites (right).

The above-discussed effect in $KO_2$ and $NaO_2$ is analogous to the Jahn-Teller effect in transition metal oxides where the energy is lowered by distortions that remove the degeneracy of the $t_{2g}$ or $e_g$ orbitals (in the common case of octahedral

coordination). In rare-earth manganite perovskites this is associated with interesting physical properties such as the colossal magnetoresistive effect [46]. Figure 1.3 shows a schematic representation of Jahn-Teller distortion in alkali superoxide ($O_2^-$) and manganite perovskite ($Mn^{3+}$) systems. The low temperature structures of alkali metal superoxides are strongly correlated with their magnetic properties.

## 1.3 Magnetic Interactions and Magnetic Order in Solids

Electron correlations/spin interactions on longer length scales result in magnetic order. Strong spin interactions can generate long-range (3D) ordered arrangements of spins. In the absence of long-range order, short-range order (1D and 2D) can exist.

Mean field theory explains ferromagnetic and antiferromagnetic interactions in terms of the presence of a molecular field originating from individual spins. This molecular field strongly interacts with a number z of nearest neighbor spins. The molecular field constant ($\lambda$) is related to Heisenberg's exchange interaction parameter ($J$) via the following equation:

$$\lambda = \frac{2zJ}{N_A g^2 \mu_B^2}. \tag{1.1}$$

Heisenberg's Hamiltonian for magnetic interactions is written as:

$$H = -\sum J_{ij} \vec{S}_i \cdot \vec{S}_j. \tag{1.2}$$

where $J_{ij} > 0$ for ferromagnetic interaction and $J_{ij} < 0$ for antiferromagnetic interaction. Ferromagnetic and antiferromagnetic interactions can arise from different mechanisms: direct exchange, superexchange, Rudderman-Kittel-Kasuya-Yoshida (RKKY) exchange, or double exchange. Direct exchange involves the direct overlap of two electron orbitals on two neighboring atoms. For small interatomic distances, according to Pauli's principle, the spins should be anti-parallel (antiferromagnetic), whereas if the atoms are further apart, the spins are parallel (ferromagnetic). There is always a balance between Coulomb energy and kinetic energy for each interatomic distance, and this determines the type of interaction [47].

Ruderman-Kittel-Kasuya-Yosida (RKKY) exchange and superexchange both involve spin interactions accommodated by intermediate atoms. RKKY exchange occurs in metals, where the medium for the exchange interactions is the conduction electrons. Superexchange interactions occur in insulators and make use of non-magnetic ions to assist spin interactions between two magnetic ions. Superexchange interaction rules based on symmetry relations and the electron occupancy, well known as the Goodenough-Kanamori-Anderson rules, have been developed [48, 49]. Superexchange interactions between magnetic superoxide anions can be

mediated by alkali metal cations. Double exchange involves the transfer of an electron between two magnetic ions with different valencies, and leads to metallic-ferromagnetic properties. Direct exchange and superexchange are the mechanisms of most interest in alkali metal superoxides and will be considered in many of the discussions of the magnetic properties of materials in this thesis. The magnetic properties of alkali metal superoxides based on their magnetic exchange interactions will be discussed in the next section.

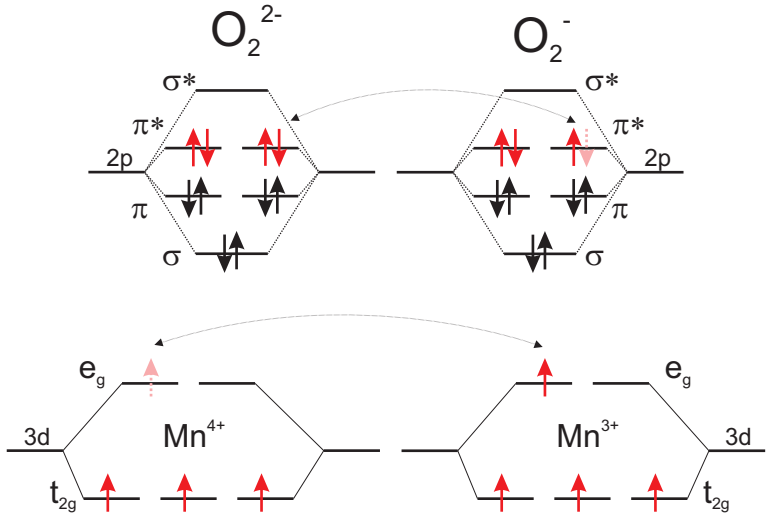


Figure 1.4. The proposed double exchange interactions in alkali metal sesquioxides in comparison to double exchange in divalently-doped rare-earth manganite perovskites.

Although direct exchange and superexchange are thought to play the main roles in the magnetic exchange interactions of alkali metal oxide compounds, the situation might be different in mixed-valent alkali oxides such as the alkali metal sesquioxides, the properties of which have not been explored much. The possibility of double exchange in the alkali metal sesquioxides, materials showing "intermediate valence state" between superoxide ($O_2^-$) and peroxide ($O_2^{2-}$), has been proposed. However, $Rb_4O_6$ and $Cs_4O_6$ are insulating materials and behave as magnetic spin glasses below 5 K [35]. It is possible that pressure (compressing the unit cell) might strengthen the magnetic exchange interactions in these sesquioxides. Pressure might be applied externally or chemically (substitution with smaller cations). Furthermore, the orthogonal arrangements of the dumbbells in $Rb_4O_6$ and $Cs_4O_6$ might prevent double exchange from occurring, which would likely be favored by a parallel arrangement. Figure 1.4 shows the possible double exchange interaction mechanism in sesquioxide compared to that of a mixed-valent manganite system involving $Mn^{3+}$ and $Mn^{4+}$ cations. If a mixed-valent alkali oxide structure could be stabilized in which double exchange is promoted, by analogy

with the divalently-doped rare-earth manganite perovskites [50], varying the oxidation state might lead to a rich phase diagram [31].

### 1.3.1 Spin Glass

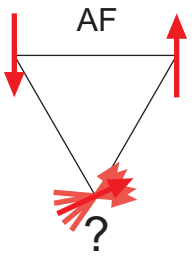


Figure 1.5. Triangular lattice showing spin frustration.

A spin glass is a system composed of frozen and disordered spins. There is no ordering, the spin orientations are random but fixed and there can be strong interactions between the spins in some cases. This frozen arrangement of spins appears below the so called freezing temperature ($T_f$). Randomness in a spin glass can be created either by site randomness or bond randomness [51]. Site randomness means that there is no spatial order of the spins, analogous to structurally amorphous compounds. Alternatively, site randomness can arise where a low concentration of a magnetic species is found in a non-magnetic lattice. Dilute magnetism leading to spin glass behavior is frequently found in intermetallic compounds. Bond randomness refers to variations in the nearest-neighbor magnetic exchange interactions, and can arise due to geometrical frustration or competing antiferromagnetic and ferromagnetic interactions. Spin glasses can be metallic (e.g. $La_{1-x}Gd_xAl_2$, $GdAl_2$, $YFe_2$), semiconducting (e.g. $Eu_xSr_{1-x}S$), or insulating (e.g. $Fe_{1-x}Mn_xTiO_3$). Examples of other spin glass compounds can be found in refs. [51] or [52]. Spin glasses can have any type of magnetic interactions, such as double exchange and RKKY interactions in metallic materials, or direct and indirect exchange (superexchange) in insulating or semiconducting compounds. A common type of spin glasses is based on geometrical frustration. For example, in a simple triangular lattice (Figure 1.5) where nearest-neighbor antiferromagnetic interactions are favorable, the direction of the third spin in the triangle is undetermined.

Experimentally, spin glasses are usually signified by irreversibility between the zero field-cooled (ZFC) and field-cooled (FC) susceptibility versus temperature curves, below which correlations between the unpaired spins become stronger. Above the splitting of the FC and ZFC curves, thermal effects induce a paramagnetic state. A peak indicating the freezing temperature ($T_f$) usually appears in

the ZFC curve. In canonical spin glasses $T_f$ should vary with $H^{2/3}$ [53]. AC susceptibility measurements can also confirm spin glass behavior. The frozen spins respond slowly to an oscillating low amplitude magnetic field. With increasing frequency the $T_f$, which appears as a peak in the real part of the AC susceptibility, shifts to higher temperature. It will be shown in Chapter 4 from AC susceptibility measurements that alkali metal oxides containing superoxide anions can exhibit glassy behavior due to clusters of ferromagnetically ordered spins with a range of sizes that interact with each other. Spin glass or cluster glass behavior can also be studied by performing time-dependent magnetization measurements. In this technique, the relaxation of the spins is monitored. Below the freezing temperature, spin glasses usually have large relaxation times. This is signified by the absence of magnetization saturation in an applied field. The strength of the spin interactions can be qualitatively determined from spin relaxation experiments. A power law dependence of the magnetization on time ($m_o t^{-\alpha}$) signifies strong magnetic interactions, whereas an exponential dependence $\left(exp(-t/\tau_o)^{\beta}\right)$ signifies weak magnetic interactions ($\alpha$ and $\beta$ are constants, and $\tau_o$ is the relaxation time).

### 1.3.2 Low-Dimensional Magnets

The spin directions in a system can be restricted to be parallel or antiparallel to each other (Ising spins) or can be free to point in any direction (Heisenberg spins). Spin interactions can be generalized by the following Hamiltonian:

$$H = -2J \sum_{i>j} \left[ a S_i^z S_j^z + b(S_i^x S_j^x + S_i^y S_j^y) \right]. \tag{1.3}$$

The Heisenberg model is obtained if $a = b = 1$, whereas $a = 1$ and $b = 0$ corresponds to the Ising model. An intermediate model is the XY-model, which is obtained if $a = 0$ and $b = 1$. In the XY-model the spins are constrained to lie only in the $xy$-plane. The XY-model is also sometimes referred to as the planar Heisenberg model. Equation 1.3 does not involve the dimensionality of the lattice. When spin interactions are limited in one (1D) or two (2D) specific spatial directions of the lattice, low-dimensional magnetism can occur. Experimental observations of low-dimensional magnetic systems are usually marked by a broad peak in the magnetic susceptibility or heat capacity versus temperature curve.

In a low-dimensional spin system the anisotropy is usually large such that magnetic interactions in the directions perpendicular to the spin-spin interaction direction can be neglected. For example, in a 1D spin chain the distance between the neighboring chains is usually relatively large such that magnetic interactions between the chains are extremely weak. An ideal S = 1/2 chain cannot exist at zero temperature due to quantum spin fluctuations, which lead to a dimerized spin-singlet state with a finite energy gap as in $CuGeO_3$ [54]. Alternatively, 3D magnetic order often arises due to magnetic interactions between adjacent spin-chains, sometimes the result of a structural distortion. For example, a second

peak in specific heat, thought to indicate the onset of long-range antiferromagnetic ordering, is observed for the spin chain compound $Cu(NH_3)_4SO_4.H_2O$ [55]. Similarly, an anomaly in the magnetic susceptibility below the 1D ordering regime in $NiCl_3(C_6H_5CH_2CH_2NH_3)$ is presumed to indicate long-range magnetic order [56]. A spin chain cannot show long-range ordering at any temperature above zero [57]. The upturn in susceptibility at temperatures well below $J/k_B$ that is often observed for S = 1/2 spin chain systems is related to non-ordered individual spins at the ends of chains that contain odd numbers of spins [58]. Paramagnetic tails can also be found in spin-chain systems that exhibit long-range 3D magnetic order at low temperature, indicating a contribution from impurities or crystal defects. In contrast to S = 1/2 chains, the zero susceptibility at T = 0 that can be found for a S = 1 spin-chain system is indicative of an excitation gap. This is derived from Haldane's presumption that half-integer spin chains are gapless and integer spin chains show a spin-excitation energy gap [59–61].

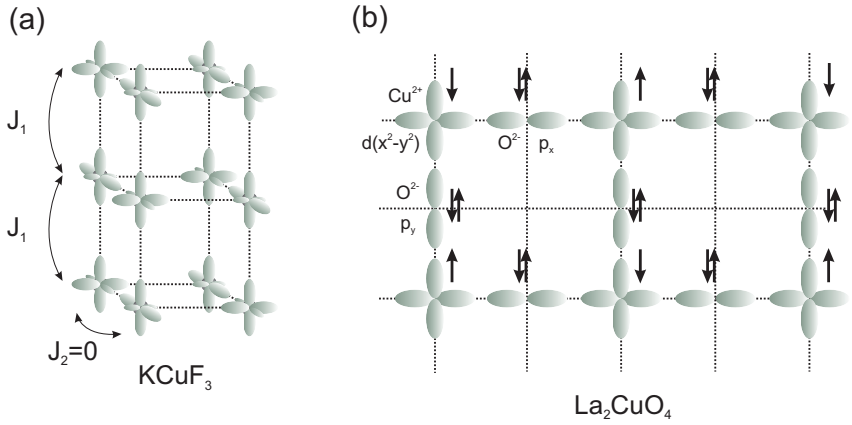


Figure 1.6. (a) One-dimensional magnetic system in $KCuF_3$; (b) Orbital ordering that leads to the two-dimensional magnetic system in $La_2CuO_4$.

Low-dimensional magnetic behavior is often a result of low structural dimensionality [56, 62–64], for example induced by long organic ligands, that suppresses magnetic exchange interactions in specific crystal directions. It is also possible to realize a 1D spin chain in a structurally 3D material, as occurs in $KCuF_3$ [65–67]. $KCuF_3$ is a perovskite that contains octahedrally coordinated $CuF_6$. The structure is pseudo-cubic, so that the distances between $Cu^{2+}$ cations are almost the same in the three principal directions of the lattice. As the Jahn-Teller effect comes into play, the orbital degeneracy of the $Cu^{2+}$ cations is removed and there are alternate distortions of the $CuF_6$ octahedra in the *ab*-plane, such that an antiferro-arrangement of the half-filled orbitals occurs. This staggered orbital configuration does not allow orbital overlap within the *ab*-plane. As a result, the

magnetic exchange interaction is confined to the *c*-direction, yielding a 1D magnetic system [65, 68]. Figure 1.6(a) shows two unit cells of $KCuF_3$. The lobes of the half-occupied $e_g$ orbitals only overlap in the *c*-direction (via fluorine $p_z$-orbitals), and as a consequence magnetic interactions appear along the *c*-direction. No magnetic interaction exists in the *ab*-plane due to the staggered arrangement of the half-filled orbitals (antiferro-orbital ordering). $KCuF_3$ is a Heisenberg spin system, so that the spins are free to point in any direction. An example of a two-dimensional system is shown in Figure 1.6(b). $La_2CuO_4$ is an antiferromagnetic S = 1/2 system where antiferromagnetic ordering in the plane arises from superexchange interactions of $Cu^{2+}$ ions mediated by oxygen ions [69]. The two-dimensionality is determined by the 2D nature of the crystal structure. A 1D orbitally-driven p-electron spin chain will be discussed in Chapter 5 of this thesis and compared with the 1D 3d-electron system $KCuF_3$.

## 1.4 Magnetic Properties of Alkali Metal Oxides

### 1.4.1 Magnetic Exchange Interactions in Alkali Metal Superoxides

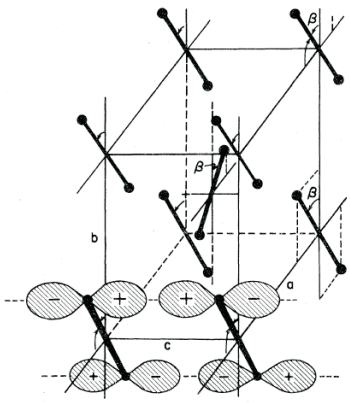


Figure 1.7. Molecular arrangement in the marcasite phase of $NaO_2$. The figure is taken from ref. [45].

In alkali metal superoxides, the direction of the magnetic moment is perpendicular to the axis connecting the two oxygen atoms [70]. The magnetic interactions in alkali metal superoxides are thus strongly correlated with the crystal structure. For example, a transition from weak 3D ferromagnetic interactions to strong 1D antiferromagnetic interactions has been suggested to occur in $NaO_2$, which occurs with a structural phase transition from an ordered pyrite to marcasite structure

[71]. The orientation of the dumbbells is the main factor that determines the magnetic interactions.

In the case of the marcasite phase of $NaO_2$, strong antiferromagnetic interactions are thought to be achieved via direct overlap of the neighboring half-filled antibonding molecular orbitals, which is made possible by the parallel arrangement of the dumbbells (see Figure 1.7). However, the magnetic properties and possible orbital ordering in $NaO_2$ have not been studied in any detail. The possibility of ferromagnetic interactions arising from superexchange between two dumbbells mediated by the alkali metal cation has also been discussed in the literature [71, 72], and is thought to follow the Goodenough-Kanamori-Anderson rules for 3d superexchange.

### 1.4.2 Magnetogyration

The spin magnetic moment in the superoxide molecule is always perpendicular to the molecular axis. Thus the dumbbells can be re-oriented by an external magnetic field, or in $KO_2$ by cooling towards the magnetic ordering transition, the so called magnetogyration effect [73, 74]. The magnetogyric phase transition from phase IV to phase VI of $KO_2$ appears at $T \approx 1.5T_N$, where $T_N = 7.1$ K is the 3D antiferromagnetic ordering temperature (see Figure 1.8). It involves a reorientation of the dumbbells such that their half-filled $\pi^*$ orbitals can overlap with the $p_z$ orbitals of $K^+$ [73], stabilizing 3D antiferromagnetic order.

### 1.4.3 Field-induced Transitions

The effect of an applied magnetic field on the re-orientation of the superoxide dumbbells has been discussed for $KO_2$ by Bosch et al. [74]. Figure 1.8 shows the magnetic phase diagram of $KO_2$. The line intersecting the horizontal axis at 10.6 K indicates the transition between the paramagnetic phase and the magnetogyric phase as described in the previous subsection. It is quite clear from the phase diagram that an applied magnetic field cannot rotate the spins in the paramagnetic phase ($T > 12.1$ K). At magnetic fields above the spin-flop (SF) phase at low temperature ($T \to 0$) the spins become aligned along the applied magnetic field direction in the paramagnetic (P) phase. This can only happen by a reorientation of the dumbbells and a first-order structural transition takes place, destroying the magnetogyric phase (VI). This is a reversal of the magnetogyric phase transition at 10.6 K that occurs on cooling in zero field. The transition from the AF (VI) to the spin-flop (SF) phase (VI) above $\sim$15 kOe occurs rather differently to a metamagnetic transition in an anisotropic system. In the latter case, a spin-flop transition leads to a ferri- or ferromagnetic state. On the contrary, a spin-flop transition in a superoxide system requires rotation of the superoxide dumbbells, which must overcome an energy barrier and is thus hindered.

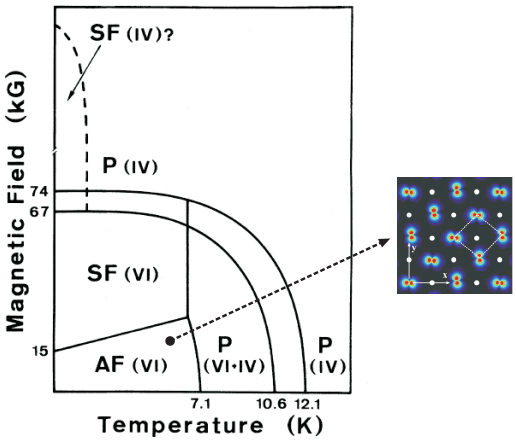


Figure 1.8. Magnetic phase diagram of $KO_2$. The 3D antiferromagnetic order in phase VI ($< 7.1$ K) is thought to be determined by ordering of half-filled $\pi_x^*$ and $\pi_y^*$ orbitals, as proposed by Nandy et al. [75]. The figures are taken from refs. [74] and [75].

## 1.5 Motivation and Outline of the Thesis

The correlation between lattice, spin, and orbital degrees of freedom in p-electron systems is an interesting subject to investigate. Apart from the well-known alkali metal oxide phases mentioned above, unexplored phases might also exist. Attempts to synthesize new alkali oxide phases and the exploration of new physical/magnetic properties will be reported. The aim of this thesis is to contribute to a better understanding of electron correlations and crystallographic behavior of the alkali metal oxides.

The experimental techniques used in this thesis will be presented in Chapter 2. In Chapter 3 I address the various phases that exist in the $RbO_x$ phase diagram. The magnetic and crystallographic behavior of these phases will be discussed. The properties of polycrystalline $RbO_2$ are slightly different from those previously reported for single crystal $RbO_2$. The magnetic interactions in $RbO_2$ will be discussed in the context of recent theoretical reports on orbital ordering in $KO_2$ and $RbO_2$.

One particular phase in the phase diagram of $RbO_x$, the novel oxygen-deficient superoxide compound $RbO_{2-\delta}$, will be discussed in detail in Chapter 4. This material shows ferromagnetic cluster glass behavior, which will be discussed in terms of possible orbital ordering configurations. The mechanisms discussed are relevant to magnetic interactions in alkali metal oxides in general.

I will present the first example of orbital-order-driven low-dimensional magnetism in a p-electron system ($CsO_2$) in Chapter 5. The superexchange interactions will be discussed in terms of the orbital ordering configuration determined by Ra-

man spectroscopy and density functional theory calculations of the phonon mode frequencies.

In chapter 6 attempts to grow thin films of $RbO_x$ will be discussed. This chapter will also discuss attempts to synthesize new phases in the potassium and cesium oxide systems.

# Bibliography


[1] de Lacheisserie, E. D. T., Gignoux, D., and Schlenker, M. *Magnetism Fundamentals*. Springer, New York, (2003).

[2] Goudsmit, S. and Kronig, R. d. L. *Die Naturwissenschaften* **13**, 90 (1925).

[3] Von Meyenn, K. *J. Magn. Magn. Mater.* **9**, 229 (1978).

[4] Pais, A. *Physics Today* **42**, 34 (1989).

[5] Johnson, M. and Silsbee, R. H. *Phys. Rev. Lett.* **55**, 1790 (1985).

[6] Prinz, G. A. *Physics Today* **48**, 58 (1995).

[7] Jedema, F. J., Filip, A. T., and van Wees, B. J. *Nature* **410**, 345 (2001).

[8] Shull, C. G. and Smart, J. S. *Phys. Rev.* **76**, 1256 (1949).

[9] Shull, C. G., Strauser, W. A., and Wollan, E. O. *Phys. Rev.* **83**, 333 (1951).

[10] Li, Y. Y. *Phys. Rev.* **100**, 627 (1955).

[11] Rajca, A., Wongsriratanakul, J., and Rajca, S. *Science* **294**, 1503 (2001).

[12] Zaidi, N. A., Giblin, S. R., Terry, I., and Monkman, A. P. *Polymer* **45**, 5683 (2004).

[13] Venkatesan, M., Fitzgerald, C. B., and Coey, J. M. D. *Nature* **430**, 630 (2004).

[14] Sundaresan, A. and Rao, C. N. R. *Nano Today* **4**, 96 (2009).

[15] Sundaresan, A. and Rao, C. N. R. *Solid State Commun.* **149**, 1197 (2009).

[16] Ohldag, H., Tyliszczak, T., Hoehne, R., Spemann, D., Esquinazi, P., Ungureanu, M., and Butz, T. *Phys. Rev. Lett.* **98**, 187204 (2007).

[17] Pan, H., Yi, J. B., Shen, L., Wu, R. Q., Yang, J. H., Lin, J. Y., Feng, Y. P., Ding, J., Van, L. H., and Yin, J. H. *Phys. Rev. Lett.* **99**, 127201 (2007).

[18] Saito, T., Nishio-Hamane, D., Yoshii, S., and Nojima, T. *Appl. Phys. Lett.* **98**, 052506 (2011).

[19] Esquinazi, P., Spemann, D., Hohne, R., Setzer, A., Han, K. H., and Butz, T. *Phys. Rev. Lett.* **91**, 227201 (2003).

[20] Yang, X., Xia, H., Qin, X., Li, W., Dai, Y., Liu, X., Zhao, M., Xia, Y., Yan, S., and Wang, B. *Carbon* **47**, 1399 (2009).

[21] Ohldag, H., Esquinazi, P., Arenholz, E., Spemann, D., Rothermel, M., Setzer, A., and Butz, T. *New J. Phys.* **12**, 123012 (2010).

[22] Barzola-Quiquia, J., Esquinazi, P., Rothermel, M., Spemann, D., Butz, T., and Garcia, N. *Phys. Rev. B* **76**, 161403 (2007).

[23] Lisenkov, S., Andriotis, A. N., and Menon, M. *Phys. Rev. B* **82**, 165454 (2010).

[24] Tombros, N., Jozsa, C., Popinciuc, M., Jonkman, H. T., and van Wees, B. J. *Nature* **448**, 571 (2007).

[25] Akahama, Y., Kawamura, H., Hausermann, D., Hanfland, M., and Shimomura, O. *Phys. Rev. Lett.* **74**, 4690 (1995).

[26] Meier, R. J. and Helmholdt, R. B. *Phys. Rev. B* **29**, 1387 (1984).

[27] Shimizu, K., Suhara, K., Ikumo, M., Eremets, M. I., and Amaya, K. *Nature* **393**, 767 (1998).

[28] Rengade, E. *Ann. Chim. Phys.* **11**, 348 (1907).

[29] de Forcand, R. *Compt. Rend.* **150**, 1399 (1910).

[30] Jansen, M. and Korber, N. *Z. Anorg. Allg. Chem.* **598**, 163 (1991).

[31] Attema, J. J., de Wijs, G. A., Blake, G. R., and de Groot, R. A. *J. Am. Chem. Soc.* **127**, 16325 (2005).

[32] Attema, J. J., de Wijs, G. A., and de Groot, R. A. *J. Phys.- Condens. Mat.* **19**, 165203 (2007).

[33] Freiman, Y. A. and Jodl, H. J. *Phys. Rep.* **401**, 1 (2004).

[34] Lide, D. R. *CRC Handbook of Chemistry and Physics (87th ed.)*. Boca Raton, FL, (2006).

[35] Winterlik, J., Fecher, G. H., Jenkins, C. A., Medvedev, S., Felser, C., Kuebler, J., Muehle, C., Doll, K., Jansen, M., Palasyuk, T., Trojan, I., Eremets, M. I., and Emmerling, F. *Phys. Rev. B* **79**, 214410 (2009).

[36] Giguere, P. A. and Harvey, K. B. *J. Am. Chem. Soc.* **76**, 5891 (1954).

[37] De Fotis, G. C. *Phys. Rev. B* **23**, 4714 (1981).

[38] Zumsteg, A., Ziegler, M., Kanzig, W., and Bosch, M. *Phys. Condens. Matter* **17**, 267 (1974).

[39] Templeton, D. H. and Dauben, C. H. *J. Am. Chem. Soc.* **72**, 2251 (1950).

[40] Rosenfeld, M., Ziegler, M., and Kanzig, W. *Helv. Phys. Acta* **51**, 298 (1978).

[41] Todd, S. S. *J. Am. Chem. Soc.* **75**(5), 1229 (1953).

[42] Hesse, W., Jansen, M., and Schnick, W. *Prog. Solid State Ch.* **19**, 47 (1989).

[43] Ziegler, M., Rosenfeld, M., Kanzig, W., and Fischer, P. *Helv. Phys. Acta* **49**, 57 (1976).

[44] Halverson, F. *J. Phys. Chem. Solids* **23**, 207 (1962).

[45] Mahanti, S. D. and Kemeny, G. *Phys. Rev. B* **20**, 2105 (1979).

[46] Mannella, N., Rosenhahn, A., Booth, C. H., Marchesini, S., Mun, B. S., Yang, S. H., Ibrahim, K., Tomioka, Y., and Fadley, C. S. *Phys. Rev. Lett.* **92**, 166401 (2004).

[47] Cullity, B. D. and Graham, C. D. *Introduction to Magnetic Materials.* John Wiley & Sons, New Jersey, (2009).

[48] Anderson, P. *Magnetism.* Academic Press, New York, (1963).

[49] Goodenough, J. *Magnetism and The Chemical Bond.* Interscience, New York, (1976).

[50] Kiryukhin, V. *New J. Phys.* **6** (2004).

[51] Mydosh, J. A. *Spin Glasses: An Experimental Introduction.* Taylor & Francis, London, (1993).

[52] Binder, K. and Young, A. P. *Rev. Mod. Phys.* **58**, 801 (1986).

[53] De Almeida, J. R. L. and Thouless, D. J. *J. Phys. A-Math. Gen.* **11**, 983 (1978).

[54] Regnault, L. P., Ain, M., Hennion, B., Dhalenne, B., and Revcolevschi, A. *Phys. Rev. B* **53**, 5579 (1996).

[55] Haseda, T. and Miedema, A. R. *Physica* **27**, 1102 (1961).

[56] Arkenbout, A. H. *Organic-Inorganic Hybrids - A Route Towards Soluble Magnetic Electronics*. PhD thesis, University of Groningen, (2010).

[57] Mermin, N. D. and Wagner, H. *Phys. Rev. Lett.* **17**, 1133 (1966).

[58] Bonner, J. C. and Fisher, M. E. *Phys. Rev. A-Gen. Phys.* **135**, A640 (1964).

[59] Haldane, F. D. M. *Phys. Rev. Lett.* **50**, 1153 (1983).

[60] Haldane, F. D. M. *Phys. Lett. A* **93**, 464 (1983).

[61] Haldane, F. D. M. *J. Appl. Phys.* **57**, 3359 (1985).

[62] Salameh, B., Yasin, S., Dumm, M., Untereiner, G., Montgomery, L., and Dressel, M. *Phys. Rev. B* **83**, 205126 (2011).

[63] Miller, J. S. and Epstein, A. J. *Chem. Commun.* , 1319 (1998).

[64] Hibbs, W., Rittenberg, D. K., Sugiura, K., Burkhart, B. M., Morin, B. G., Arif, A. M., Liable-Sands, L., Rheingold, A. L., Sundaralingam, M., Epstein, A. J., and Miller, J. S. *Inorg. Chem.* **40**, 1915 (2001).

[65] Kadota, S., Yamada, I., Yoneyama, S., and Hirakawa, K. *J. Phys. Soc. Jap.* **23**, 751 (1967).

[66] Ikeda, H. and Hirakawa, K. *J. Phys. Soc. Jap.* **35**, 722 (1973).

[67] Hirakawa, K. and Kurogi, Y. *Prog. Theor. Phys.* **46**, 147 (1970).

[68] Satija, S. K., Axe, J. D., Shirane, G., Yoshizawa, H., and Hirakawa, K. *Phys. Rev. B* **21**, 2001 (1980).

[69] Shirane, G., Endoh, Y., Birgeneau, R. J., Kastner, M. A., Hidaka, Y., Oda, M., Suzuki, M., and Murakami, T. *Phys. Rev. Lett.* **59**, 1613 (1987).

[70] Labhart, M., Raoux, D., Kanzig, W., and Bosch, M. A. *Phys. Rev. B* **20**, 53 (1979).

[71] Mahanti, S. D. and Khan, A. U. *Solid State Commun.* **18**, 159 (1976).

[72] Kim, M., Kim, B. H., Choi, H. C., and Min, B. I. *Phys. Rev. B* **81**, 100409 (2010).

[73] Lines, M. E. and Bosch, M. A. *Phys. Rev. B* **23**, 263 (1981).

[74] Bosch, M. A., Lines, M. E., and Labhart, M. *Phys. Rev. Lett.* **45**, 140 (1980).

[75] Nandy, A. K., Mahadevan, P., Sen, P., and Sarma, D. D. *Phys. Rev. Lett.* **105**, 056403 (2010).